First Exclusive Measurement of Deep Virtual Compton Scattering off ^{4}He: Toward the 3D tomography of nuclei

M. Hattawy,[1,2] R. Dupré,[1,2] N.A. Baltzell,[1,3] and K. Hafidi[1,*]

(The CLAS Collaboration)

[1] *Argonne National Laboratory, Argonne, Illinois 60439*
[2] *Institut de Physique Nucléaire, CNRS/IN2P3 and Université Paris Sud, Orsay, France*
[3] *Thomas Jefferson National Accelerator Facility, Newport News, Virginia 23606*

(Dated: January 19, 2017)

We report the first exclusive measurements of deeply virtual Compton scattering (DVCS) off a nucleus, where all the products of the reaction including the recoil ^{4}He nucleus were detected. The experiment was performed using the Jefferson Lab CEBAF Large Acceptance Spectrometer (CLAS) enhanced with a radial time projection chamber (RTPC) to detect the recoiling ^{4}He nuclei. We measure large beam spin asymmetries comparable to the proton's ones and extract in a model independent way, the single chirally-even generalized parton distribution of the ^{4}He nucleus. These are pioneering measurements and will lead the way toward the 3D imaging of the partonic structure of nuclei.

PACS numbers: Valid PACS appear here

A wealth of information on the quantum chromodynamics (QCD) structure of hadrons lies in the correlations between the momentum and spatial degrees of freedom of the fundamental constituent partons, quarks and gluons. Such correlations are accessible via the generalized parton distributions (GPDs). The GPDs correspond to the coherence between quantum states of different (or same) helicity, longitudinal momentum, and transverse position. In an impact parameter space, they can be interpreted as a distribution in the transverse plane of partons carrying a certain longitudinal momentum [1–3]. A crucial feature of GPDs is the access to the transverse position of partons which, combined with their longitudinal momentum, leads to the total angular momentum of partons [4]. Deep virtual Compton scattering (DVCS) corresponding to hard exclusive electroproduction of a real photon, which is considered as the cleanest probe to access GPDs and thus study the 3D imaging of nucleons and nuclei.

DVCS measurements have been the focus of a worldwide effort [5–15] involving several accelerator facilities such as Jefferson Lab (JLab), HERA and CERN. The vast majority of the experiments focused on the study of the nucleon's structure. The deuterium was also investigated at HERMES and JLab [16] mainly as a neutron target. However, studying the 3D imaging of the nucleon is a very important goal, understanding how these distributions are modified to provide the binding and structure in a nucleus is as fascinating of a question and an integral part of our quest of using QCD to explore nuclear matter.

A DVCS process on a nuclear target differ from single nucleon scattering in providing access to the measure two DVCS channels. In the coherent DVCS channel, the target nucleus remains intact and recoils as a whole while emitting a real photon ($eA \rightarrow e'A'\gamma$), allowing to measure the nuclear GPDs of the target. In the incoherent channel, the nucleus breaks up and the DVCS takes place on a bound nucleon that emits the final photon ($eA \rightarrow e'N'\gamma$ X), enabling the GPDs measurement of the bound nucleons and to study the medium modifications of the nucleons in the nuclear medium via the GPDs. Figure 1 illustrates the dominant mechanism for the coherent DVCS channel on ^{4}He. At sufficiently large squared electron momentum transfer Q^2 $(= -(k-k')^2)$ and small squared momentum transfer t $(= (p-p')^2)$, the QCD factorization theorem predicts that the DVCS handbag diagram can be factorized into two parts, hard and soft parts [17, 18]. The hard part includes photons-quark interaction and it is calculable through perturbative methods, while the soft/non-perturbative part is parametrized in terms of GPDs, which embed the partonic structure of the hadron.

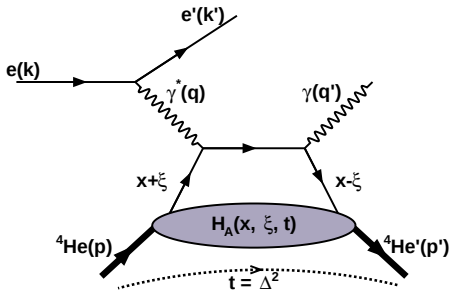

FIG. 1: Deep virtual Compton scattering process in the handbag approximation.

*corresponding author: kawtar@anl.gov

The GPDs are defined for each quark flavor and gluon as matrix elements of the light cone operators [19], describing the transition between the initial and final states of a hadron. The GPDs depend on two longitudinal momentum fraction variables (x, ξ) and on the momentum transfer t to the target. x is the average longitudinal momentum fraction of the parton involved in the process and ξ is the longitudinal fraction of the momentum transfer t, which is related to the Bjorken variable x_B: $\xi \approx \frac{x_B}{2-x_B}$, where $x_B = \frac{Q^2}{2M\nu}$ with the proton mass M and $\nu = E_e - E_{e'}$. The GPDs x variable cannot be measured experimentally in a DVCS reaction. Hence, we measure the their convolutions on x, the so-called Compton Form Factors (CFF) [20]. In a DVCS process, the number of GPDs needed to parametrize the partonic structure of a hadron depends on the different configurations between the spin of the hadron and the helicity direction of the struck quark. Therefore, the partonic structure of spin zero nuclei, such as ^4He and ^{12}C, is parametrized by only one GPD ($H_A(x,\xi,t)$) at leading twist, while 4 GPDs arise in the nucleon case. In this work, we have chose the ^{4}He nucleus as our target of interest because of it's spinless nature and it shows a clear EMC effect [21], in addition of having a high density and it is a well-known few-body system.

The study of nuclear DVCS is still in its infancy due to the challenging detection of the low-energy recoil nuclei in fixed target experiments. Until very recently, the HERMES experiment [22] was the only one to measure DVCS off heavier nuclei such as ^{4}He, N, Ne, Kr and Xe, where only the scattered electron and the real photon are detected. In this paper, we report the first exclusive measurements of the coherent DVCS channel off ^{4}He where all products of the reaction are detected including the recoiling ^{4}He nucleus. Following this exclusive measurement, the ^{4}He CFF ($\mathcal{H}_A$) will be extracted experimentally in a fully model independent way for the first time ever. The incoherent DVCS channel measurement from the same data set in in preparation and will reported in another publication.

The experiment, CLAS-EG6, took place the experimental Hall-B of Jefferson labortory (JLab) in 2009. JLab delivers a nearly 100% duty factor, 6 GeV linearly polarized electrons into three experimental halls. The data were collected over three months via projecting a 6.064 GeV longitudinally ploarized beam, (83% polarization), on a 6 atm gasous ^{4}He target, 20 cm long. The CEBAF Large Acceptance Spectrometer (CLAS) was upgraded during the CLAS-EG6 running. This detector is large acceptance covering nearly 2π and is composed of drift chambers, Cherenkov counters, scintillator counters and an electro-magnetic calorimeter. It allows to detect accurately electrons which provide the trigger for the experiment. It is complemented for DVCS experiments with an inner electro-magnetic calorimeter made of PbWO crystals to detect the photons emitted at low

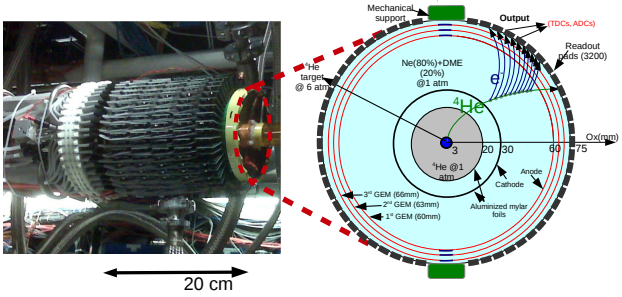

FIG. 2: Left: A picture of the CLAS-EG6 RTPC before insertion into the solenoid. Right: A cross section of the CLAS-EG6 RTPC perpendicular to the beam direction. An illustration of a ^{4}He track originating from the pressurized straw target is shown along with the electrons produced in the drift region.

angle and with a solenoid to keep the Moller electrons produced along the beam line to get into our detectors.

In order to ensure the coherence of the process, we also detect the recoiling helium-4 nuclei. We built a small and light radial time projection chamber (RTPC) to detect recoiling helium nuclei down to energies of few MeVs. The chamber, shown in figure 2, is surrounding the gaseous target filled with 6 atm helium-4 and is 20 cm long with a 3 cm radial drift length. The detector was specifically calibrated for helium-4 nuclei using elastic scattering produced with a 1.2 GeV electron beam. To ensure that the process is exclusive, we apply cuts on several kinematic variables (figure 3) such as missing energy, mass and momentum. The cuts are chosen to represent consistently 3 half width at half maximum in order to avoid any bias in the selection.

we extract the GPD H in a model independent way (figure 6). This is possible using the beam-spin asymmetry (A_{LU}) expression for spin-zero target at leading twist [**?**]:

$$A_{LU}(\phi) = \frac{\alpha_0(\phi)\,\Im m(\mathcal{H}_A)}{\alpha_1(\phi) + \alpha_2(\phi)\,\Re e(\mathcal{H}_A) + \alpha_3(\phi)\left(\Re e(\mathcal{H}_A)^2 + \Im m(\mathcal{H}_A)^2\right)} \quad (1)$$

where $\Im m(\mathcal{H}_A)$ and $\Re e(\mathcal{H}_A)$ are the imaginary and real parts of the CFF $\mathcal{H}_A$ associated to the GPD H_A. The α_i's are ϕ-dependent kinematical factors that depend on the nuclear form factor F_A and the independent variables

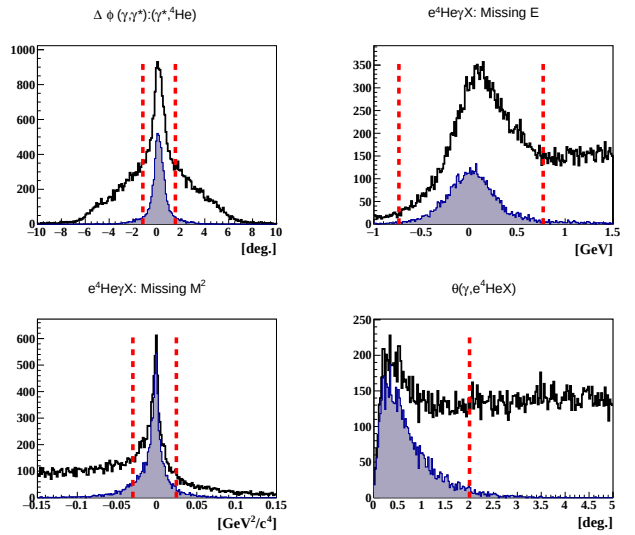

FIG. 3: The coherent DVCS exclusivity cuts. The black distributions represent the coherent DVCS events candidate. The shaded distributions represent the events which passed all the exclusivity cuts except the quantity plotted. The vertical red lines represent 3σ cuts.

Q^2, x_B and t. These factors are simplified as:

$$\alpha_0(\phi) = \frac{x_A(1+\epsilon^2)^2}{y} S_{++}(1)\sin(\phi) \quad (2)$$

$$\alpha_1(\phi) = c_0^{BH} + c_1^{BH}\cos(\phi) + c_2^{BH}\cos(2\phi) \quad (3)$$

$$\alpha_2(\phi) = \frac{x_A(1+\epsilon^2)^2}{y}\left(C_{++}(0) + C_{++}(1)cos(\phi)\right) \quad (4)$$

$$\alpha_3(\phi) = \frac{x_A^2 t(1+\epsilon^2)^2}{y}\mathcal{P}_1(\phi)\mathcal{P}_2(\phi)\cdot 2\frac{2-2y+y^2+\frac{\epsilon^2}{2}y^2}{1+\epsilon^2} \quad (5)$$

Where $S{+}{+}(1)$, $C_{++}(0)$, and $C_{++}(1)$ are the Fourier harmonics in the leptonic tensor. Their explicit expressions can be found in .

We thank the staff of the Accelerator and Physics Divisions at Jefferson Lab for making this experiment possible.

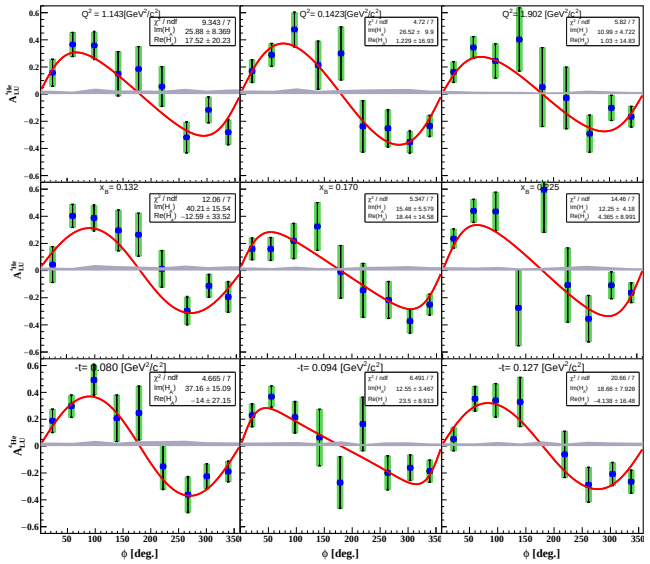

FIG. 4: The coherent A_{LU} as a function of ϕ in Q^2(top panel), x_B (middle panel), and $-t$ (bottom panel) bins. The error bars represent the statistical and the systematic uncertainties added quadratically, shown on top in green are error bars representing only the statistical uncertainties. The brown bands represent the systematic uncertainties, including the normalisation systematic uncertainties. The red curves represent fits in the form of equation 1.

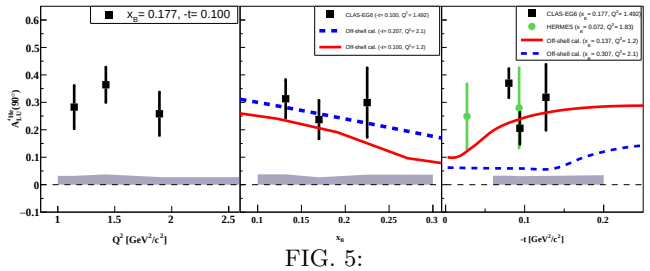

FIG. 5:

[1] M. Burkardt, Phys. Rev. D **62**, 071503 (2000) Erratum: [Phys. Rev. D **66**, 119903 (2002)]

[2] M. Diehl, Eur. Phys. J. C **25**, 223 (2002) Erratum: [Eur. Phys. J. C **31**, 277 (2003)]

[3] A. V. Belitsky and D. Mueller, Nucl. Phys. A **711**, 118 (2002)

[4] M. Burkardt, Phys. Rev. D **72**, 094020 (2005)

[5] S. Stepanyan *et al.* [CLAS Collaboration], Phys. Rev. Lett. **87**, 182002 (2001).

[6] A. Airapetian *et al.* [HERMES Collaboration], Phys. Rev. Lett. **87**, 182001 (2001); JHEP **1207**, 032 (2012); JHEP **1006**, 019 (2010); JHEP **0806**, 066 (2008); Phys. Lett. B **704**, 15 (2011); Phys. Rev. D **75**, 011103 (2007); JHEP **0911**, 083 (2009); Phys. Rev. C **81**, 035202 (2010); JHEP **1210**, 042 (2012).

[7] S. Chekanov *et al.* [ZEUS Collaboration], Phys. Lett. B **573**, 46 (2003).

[8] A. Aktas *et al.* [H1 Collaboration], Eur. Phys. J. C **44**, 1 (2005).

[9] S. Chen *et al.* [CLAS Collaboration], Phys. Rev. Lett. **97**, 072002 (2006).

[10] C. Muñoz Camacho *et al.* [Jefferson Lab Hall A Collaboration], Phys. Rev. Lett. **97**, 262002 (2006).

[11] F.X. Girod *et al.* [CLAS Collaboration], Phys. Rev. Lett. **100**, 162002 (2008).

[12] G. Gavalian *et al.* [CLAS Collaboration], Phys. Rev. C **80**, 035206 (2009).

[13] E. Seder *et al.* [CLAS Collaboration], Phys. Rev. Lett. **114**, 032001 (2015).

[14] S. Pisano *et al.* [CLAS Collaboration], Phys. Rev. D **91**, 052014 (2015).

[15] H. S. Jo *et al.* [CLAS Collaboration], Phys. Rev. Lett.

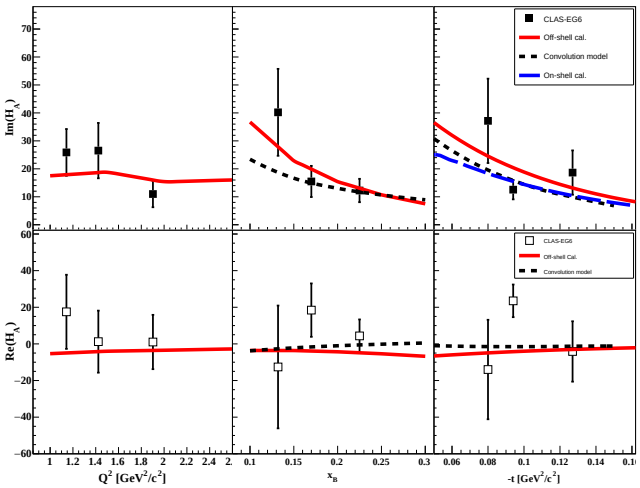

FIG. 6: The model-independent extraction of the imaginary (blue points) and real (red points) parts of the ^{4}He CFF $\mathcal{H}_A$, as functions of Q^2 (on the top right), x_B (on the top left), and t (on the bottom).

115, no. 21, 212003 (2015)
[16] M. Mazouz *et al.* [Jefferson Lab Hall A Collaboration], Phys. Rev. Lett. **99**, 242501 (2007)
[17] A. Freund and J.C. Collins, Phys. Rev. D **59**, 074009 (1998)
[18] X.-D. Ji and J. Osborne, Phys. Rev. D **58**, 094018 (1998)
[19] A. V. Belitsky and A. V. Radyushkin, Phys. Rept. vol. 418 (2005)
[20] M. Guidal, H. Moutarde and M. Vanderhaeghen, Rept. Prog. Phys. **76**, 066202 (2013)
[21] J. Seely *et al.* Phys. Rev. Lett. **103**, 202301 (2009)
[22] F. Ellinghaus *et al.* [HERMES Collaboration], AIP Conf. Proc. **675**, 303 (2003)